Dynamics of flame propagation using laser-induced spark initiation: Ignition energy measurements

J. A. Syage, E. W. Fournier, R. Rianda, and R. B. Cohen
Aerophysics Laboratory, The Aerospace Corporation, P. O. Box 92957, Los Angeles, California 90009

(Received 30 December 1987; accepted for publication 29 March 1988)

A method is described for measuring low-energy ignition of combustible mixtures using nanosecond and picosecond laser-induced breakdown. Ignition studies are reported for homogeneous H_2/air mixtures. The extent of flame inhibition in H_2/air was investigated as a function of CO_2 concentration. Our electrodeless spark ignition results are compared with earlier work using electric discharge ignition. A simple model for flame ignition is advanced, based on the temporal and energy density characteristics of the source energy. Implications of laser-induced spark ignition in homogeneous fuel mixtures to the molecular dynamics of flame propagation are discussed.

I. INTRODUCTION

Despite the enormous literature that exists on flame chemistry,[1,2] the properties of the ignition process are not well understood on a molecular level. We have initiated studies to probe the dynamics of flame propagation from incipient formation to stages in the evolution of the flame front that give rise to deflagration, detonation, or extinction. It is expected that a detailed understanding of the time-dependent kinetics and energy transfer mechanisms at the flame front (i.e., the preheat and reaction zone interface) will prove vital in learning how to enhance or inhibit flame propagation. In recent years, a number of important laser diagnostic techniques have been applied to fuel systems in order to measure reactive intermediate (usually OH) densities and vibrational distributions.[3–10] These studies have provided important information about flame temperatures and collisional deactivation. However, these investigations invariably considered stable flames under steady state conditions. In the present case, we are interested in the time evolution of flame propagation during the critical early stages of the minimal flame when the conditions leading to propagation versus extinction are most sensitive to the interplay of energy and mass flow interactions.

The use of laser-induced breakdown to initiate the spherical propagation of the flame front was investigated as an alternative to the use of electrode discharge,[11,12] which is considered to be too intrusive for these studies. The effects of heterogeneous catalysis, ablation of material, and interference with the expanding flame front are particular concerns in using electric discharge to study properties of ignition. The use of laser-induced breakdown to initiate spark ignition provides a well-defined source of energy localized in free space. The challenge is to generate and measure the low-energy spark and to examine whether wavelength and laser pulse duration affect the coupling of the spark energy to the combustion wave. It may be argued that ignition is not sensitive to laser pulse widths that are much shorter than the time scale for the primary kinetic steps in combustion, in which case, the governing factor to laser ignition is whether breakdown has occurred and how much energy is absorbed in the spark.

The properties of laser-induced breakdown (or optical discharge) have been studied intensely.[13,14] Several groups reported studies involving laser-induced spark ignition[15–20]; however, in only one case was an attempt made to systematically control the energy of the laser spark[15] to measure ignition energies. A number of other studies have investigated photochemical ignition[21–24]; however, this process involves resonant single-photon or multiphoton dissociation to generate a reactive species,[23–25] as opposed to nonresonant laser-induced breakdown which is considered to serve as a thermal ignition source. Naturally, the extent to which laser-induced ignition is a thermal process is a critical concern.

The dynamics of flame initiation and propagation are sensitive functions of the mechanisms by which the source energy couples into the surrounding medium of the incipient combustion wave. A comprehensive treatment of this problem is complex. Instead, we shall identify and model the problem of flame initiation and extinction to emphasize the temporal properties of the ignition energy source. The kinetics of the combustion defines the relevant time scale. Hence, the distinction between short laser pulses of different duration is less important than that between short laser pulses and other ignition sources (e.g., electric discharge) where the energy is deposited on a time comparable to the reaction kinetics. Consideration will also be given to source geometry and turbulence. The treatment is intended to draw together simple concepts relating to source energy density, duration, and dissipation processes.

We have organized the paper as follows. In Sec. II, we describe our experimental method for generating and measuring laser-induced spark energies, for measuring ignition energies, and for recording time-resolved emission and pressure measurements. We present our results in Sec. III. Light-scattering experiments are described to demonstrate the accuracy of the spark energy measurements (Sec. III A). Ignition energy measurements for H_2/air and H_2/air/CO_2 mixtures are presented as a function of relative concentration, laser pulse duration, and wavelength (Sec. III B). A comparison of these results is made to previous electric-discharge ignition measurements. Time-resolved measure-

 0021-8979/88/151499-09$02.40

ments of pressure and OH luminescence in our adiabatic reaction cell are reported (Sec. III C). In Sec. IV, we discuss the role of source energy duration and density on the ignition process, as well as the role of energy dissipation that competes with the ignition process. We consider two divergent models for ignition. A homogeneous hot-gas model is considered, which assumes that the necessary energy for ignition is deposited in the most favorable manner (Sec. IV A). Ignition energies are then calculated and compared to the present laser spark and the previous electric-discharge results. We then consider how the minimum ignition energy is affected if the source energy is modeled as an instantaneous point source (Sec. IV B). This model, which has a physical basis to laser spark ignition, calculates the evolution of a blast wave and the resulting dissipation of energy. Finally, we consider whether the release of chemical energy in the early flame can enhance the ignition process to an extent that would explain the anomalously low ignition energies measured by electric discharge (Sec. IV C). Finally, the conclusions of this paper are summarized in Sec. V.

II. EXPERIMENT

A schematic of the experimental apparatus is presented in Fig. 1. The reaction chamber consists of a 4-in. conflat cube that has been Teflon coated to eliminate metal surface interactions. The reaction chamber is connected to a 5-l evacuated buffer chamber and separated by a 0.75-in.-diam Al foil membrane. Ignitions are therefore quenched when the pressure wave reaches the chamber walls and punctures the Al foil membrane leading to the vacuum. The purpose of this arrangement is to safeguard against transitions to detonation. Four sides of the reaction chamber are equipped with three 2-in. focal length quartz lenses and a quartz plate that are flange mounted and act as windows. Two lenses serve as the entrance and exit windows for the laser pulse; the remaining lens and window, which are orthogonal to the laser axis, serve for detection of scattered light and spark and/or flame emission, respectively. Detection devices are described below. The remaining sixth side allows installation of a pressure transducer and fast thermocouple detector.

The laser-induced ignition is achieved by focusing the output of the second or third harmonic of a Nd-YAG laser (Quantel QY471) operating either as a Q-switched nanosecond (ns) laser or a pulse mode-locked picosecond (ps) laser. The Q-switched arrangement is of conventional design, delivering pulse widths of approximately 12 ns (532 nm) or 9 ns (355 nm). The ps pulses are derived from a pulsed active/passive mode locker that creates a short train of pulses. A single pulse is selected and further amplified before passing through the harmonic-generating crystals. Pulse widths are about 50 ps (1064 nm), 35 ps (532 nm), and 25 ps (355 nm).

Spark energy measurements are made by splitting off about 10% of the incident laser pulse and comparing its energy relative to the pulse transmitted through the reaction chamber after spark formation. The two energy levels are calibrated in the absence of breakdown by evacuating or reducing the pressure of the reaction chamber. The attenuation of the transmitted light, in the case of breakdown, is attributed to the absorption of energy by the spark. The transmitted and reference pulse energies are measured using Laser Precision pyroelectric energy meters, which in turn are calibrated to a Scientech thermopile energy meter. Spark energies are controlled by attenuating the laser output, using either a rotatable polarizer or a wedge-prism beam attenuator (Newport 935-10). These devices are placed after the YAG amplifier stage so as not to affect the beam profile.

Time-resolved emission spectra of the luminous OH radical in the flame were recorded using a 308-nm interference filter (12-nm bandwidth) and a 1P28 photomultiplier tube. The emission signal was digitized using a 100-MHz, 8-bit transient digitizer. Absolute measurements of scattered laser light at right angles to the laser direction were made, using a calibrated energy meter (see above). Relative anisotropic distributions were obtained by mounting a fiber optic onto a

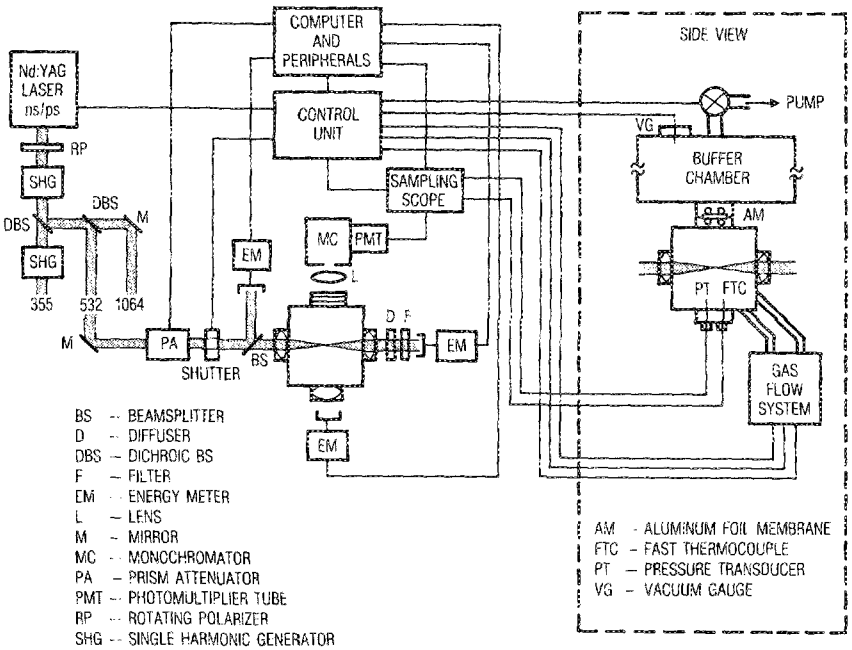

FIG. 1. Schematic of experimental apparatus viewed from the top and from the side (insert), along with associated excitation and detection components.

rotation stage. Time-resolved pressure measurements were made at the wall of the chamber (approximately 5 cm from the center where ignition occurs) using a piezoelectric pressure transducer. The pressure signal was digitized in a manner similar to the emission measurements.

The laser-induced ignition studies made use of a gas handling system that delivers a precise and homogenous combustion mixture prior to the introduction of a single laser pulse to initiate the combustion. We have automated this operation by building a digital control unit and computer interface that controls the necessary sequence of events. Specific proportions of up to four gases are controlled using mass flow controllers, and are allowed to circulate through the reaction chamber for a time sufficient to reach equilibrium (about 1 min). The control unit then closes the circulating valves and the fuel flow controller opens a bypass valve, and begins a 1.6-s delay (4-bit counter at 10 Hz). A shutter is then triggered to allow a single laser pulse to enter the chamber to create the spark. The transmitted and reference energy meter-readings are digitized by an A/D card in an IBM PC and the spark energy computed and displayed in real time. For minimum ignition energy measurements, it is common to use low spark energies that do not ignite the mixtures; consequently (after a 5-s delay) the above sequence is repeated until an ignition occurs. Ignitions are detected by monitoring the pressure increase in the buffer chamber due to the rupturing of the Al foil membrane, in which case the control unit terminates the timing sequence and initiates an evacuation sequence. The occurrence of ignition is also evident by detecting OH luminescence or pressure reaching the chamber walls.

III. RESULTS

The object of this work is to show that ignition energies can be measured using laser-induced sparks and to understand how specific sources of energy influence the ignition process. We first examine our method for measuring spark energies to show that the attenuation of light through the reaction cell is due to absorption by the spark and not scattering. We then compare our laser-ignition energy results as a function of pulse duration (~ 10 ns vs ~ 30 ps) and wavelength to electric-discharge ignition results.

A. Spark energy measurements

The accuracy of the method for measuring spark energy, described in Sec. II, is examined here. The principal source of energy loss in the transmitted light, other than spark absorption, is the scatter of laser light by the developing spark plasma. This was measured perpendicular to the incident laser axes of propagation $\hat{x}$ and polarization $\hat{E}$, using a calibrated energy meter and $f/2.8$ collection optics. The data are expressed as the total scattered light by assuming an isotropic distribution throughout the scattering volume. The results are presented in Fig. 2(a) as a function of laser pulse energy. The scattered light in vacuum is assumed to be stray light reflected off windows. The additional scattered light in air may be due to Rayleigh scattering or scattering off the spark. In either case, the fraction of scattered light (assuming an isotropic distribution) to absorbed light [Fig. 2(a)] is sufficiently small (<0.001) to be of negligible concern in the spark energy determinations.

The possibility for large anisotropies in the angle of light that is scattered by the plasma was investigated by measuring the relative angular distribution $f(\theta)$ of scattered light in the two planes parallel to $\hat{x}$. The results in Figs. 2(b) and 2(c) (where $\theta = 0$ for the $\hat{x}$ direction) show that there are no adversely strong lobes as a function of θ, although scattering at small angles was difficult to measure owing to other sources of scattered light when viewing down the optical train. Recent results on laser beam diffraction in low-energy sparks[26] indicate that as much as 10% of the incident light is diffracted; however, it is contained within the range $\theta < 14°$. Since our collection optics for transmitted light has a solid angle of detection comparable to this value, losses due to diffraction are considered insignificant. Hence, the energy loss of the transmitted light through the spark can be considered to be absorbed, and therefore accounts for the energy of the spark.

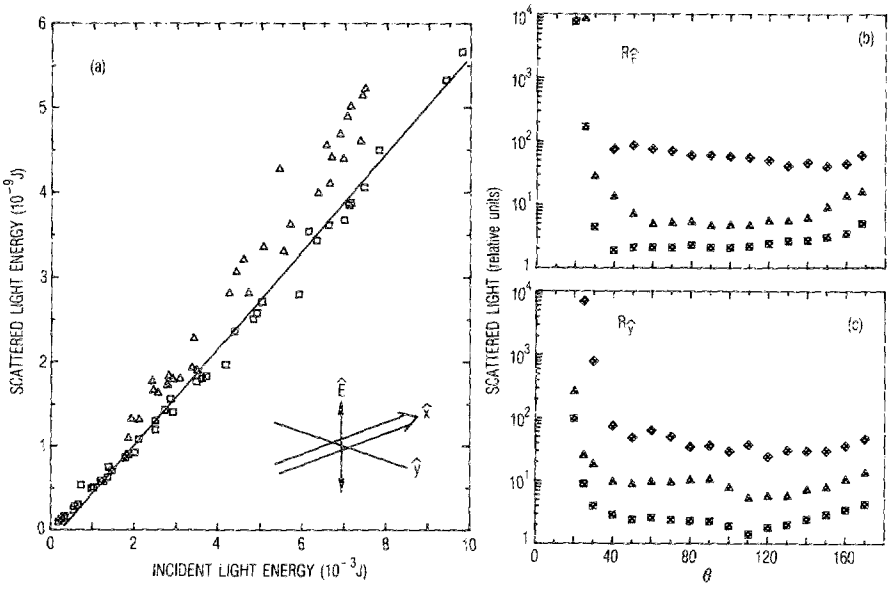

FIG. 2. (a) Total scattered laser light (532-nm, 30-ps pulse width) in vacuum (□) and in air (△) assuming an isotropic distribution. The line represents the best linear fit to the vacuum measurements. Deviations from linearity for the air sample occur as a result of scattering off the spark. (b), (c) Anisotropic distribution of scattered laser light off the spark, measured in planes parallel to $\hat{x}$; (b) rotation about the axis $\hat{E}$; and (c) rotation about the axis $\hat{y}$ [see insert in (a)]. The symbols refer to pulse energies of 0.5 mJ (▩), 2.0 mJ (▲), and 6.0 mJ (◆).

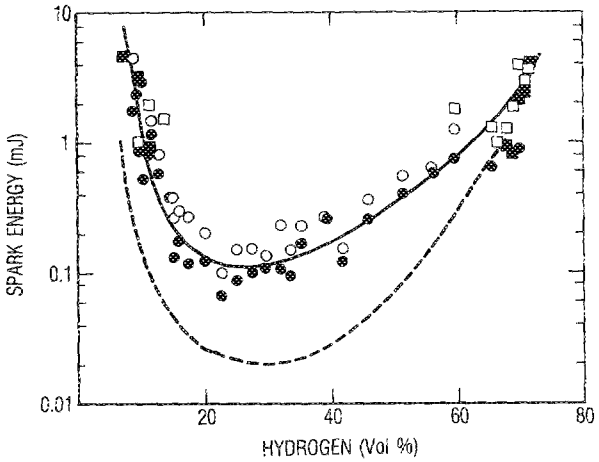

FIG. 3. Minimum ignition energy measurements for H_2/air mixtures using 355-nm nanosecond (■,□) and 532-nm picosecond (○,●) laser-induced sparks. Solid symbols represent highest-energy nonignitions, and open symbols represent lowest-energy ignitions. The curve through the data is drawn for visualization. Electric-discharge results of Lewis and Von Elbe (Ref. 2) are indicated by a dashed line.

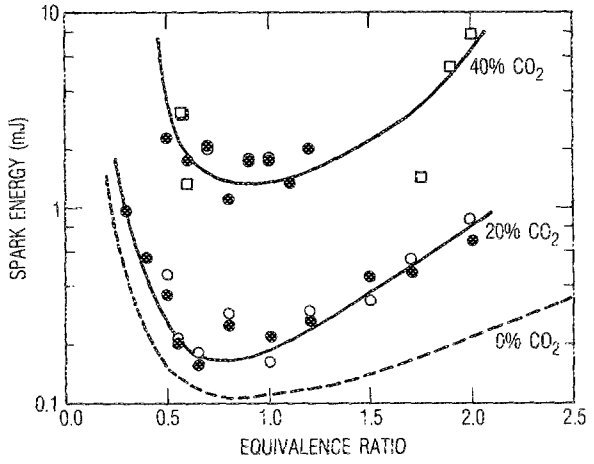

FIG. 4. Minimum ignition energy measurements for H_2/air/CO_2 mixtures showing the effect of CO_2 dilution. Symbols are described in Fig. 3. The dashed line represents the data of Fig. 4 for no CO_2 dilution.

B. Minimum ignition energy measurements

Minimum ignition energies were measured for H_2/air using ns and ps laser-induced sparks. The shorter ps pulses were essential for measuring the low-energy ignition levels for H_2/air near stoichiometry. The higher peak powers and lower total pulse energies compared to ns pulses extended the practical low-energy range for spark formation from 0.5 mJ to 20 μJ. The measured minimum ignition energy results for H_2/air mixtures are plotted in Fig. 3, using 532-nm ps pulses and 355-nm ns pulses as the ignition source. Only the highest-energy nonignition and lowest-energy ignition results for each fuel ratio are represented. However, all the data attest to reproducible and smooth transitions to ignition as a function of laser-induced spark energy. The results of Lewis and von Elbe[2] using electric discharge are included in Fig. 3 and indicate a discrepancy between the two sets of results that decreases toward the upper ignition limit. There is also a slight disparity between the ns and ps results in the upper ignition limit, but not of a magnitude that is significant compared to the uncertainty of the measurements. The minimum in the energy curve occurs to the lean side of stoichiometry (0.11 mJ at 23% H_2 or an equivalance ratio of $\phi = 0.8$). This behavior is characteristic of light, highly diffusive fuels (e.g., H_2) which tend to replenish burned fuel at the spherical flame front during the critical early stages of the minimal flame.[1,2]

The effect of CO_2 dilution on the H_2/air ignition process by laser-induced spark ignition was investigated. The results for 20% and 40% CO_2 content are compared to the undiluted H_2/air results in Fig. 4. Not shown are 1064-nm ps data for mixtures near stoichiometry, which reveal no significant differences from the 532-nm data. Ignition energies for hexane and 1,1'-dimethyl hydrazine in air were also measured.[27] However, our initial flow system did not permit us to verify the actual concentrations in the reaction cell for these condensable fuels. Hence we report only the minimum energies in the ignition curves: 0.56 mJ for hexane and 0.44 mJ for 1,1'-dimethyl hydrazine. The only previous measurement is an electric-discharge study of hexane/air by Lewis and Von Elbe[2] in which they obtained a minimum energy of 0.21 mJ for an equivalence ratio of $\phi = 1.6$.

C. Flame pressure, velocity, and OH luminosity

Time-resolved measurements of the flame luminosity due to the $X^2\Pi_i \leftarrow A^2\Sigma^+$ emission of OH were recorded, using a field of view that encompassed approximately the entire reaction volume. The results for stoichiometric H_2/air are compared in Fig. 5 with time-resolved pressure readings measured at the wall of the chamber. The time at which the peak intensities occur for emission and pressure are in good

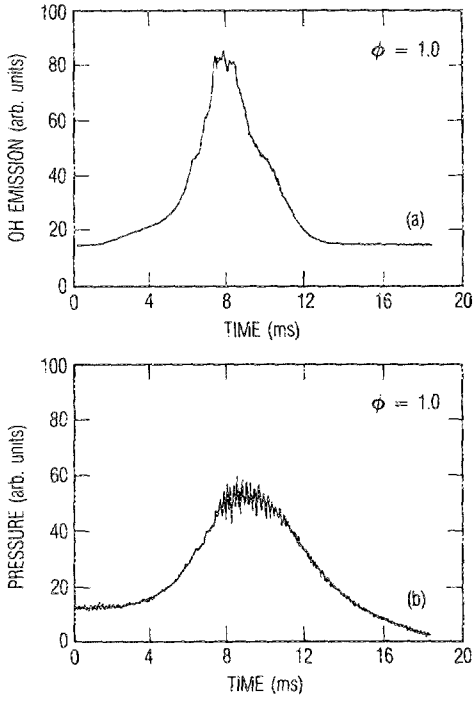

FIG. 5. Time-resolved measurements of (a) flame luminosity ($X^2\Pi_i \leftarrow A^2\Sigma^+$ emission of OH) and (b) pressure. The emission was detected over the entire reaction volume, and the pressure at the chamber wall.

agreement, a trend also observed for other fuel mixture ratios. The correspondence occurs since the luminous spherical surface area of the flame front is greatest when it reaches the chamber wall. The average flame speed at stoichiometry of $\sim 10^3$ cm/s is about a factor of 5 greater than the 1-atm constant pressure laminar burning velocity.[2] In our constant volume chamber, the temperature and pressure of the unburned gas increase as the flame progresses, due to adiabatic compression; hence, the burning velocity increases with time.[2,28] The velocity of the luminous wave front has previously been studied under very different energy and pressure regimes.[29]

Emission and pressure traces exhibited decreasing rise times to the rich side of stoichiometry which is consistent with the trend in burning velocity in laminar flames.[2] Evidence for oscillatory behavior in the combustion process is suggested by periodic structure in the pressure profile for $\phi = 1.0$ in Fig. 5(b). Leaner mixtures exhibited much stronger oscillations in both the emission and pressure traces.[30]

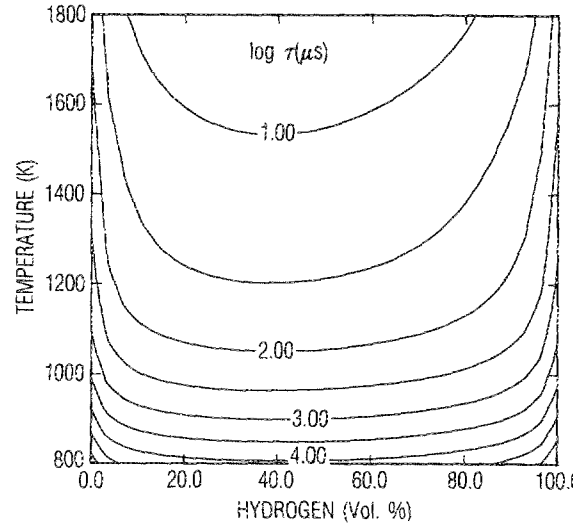

FIG. 6. Calculated dependence of the chemical induction time for H_2/air combustion as a function of temperature and H_2 percentage by volume at 1 atm.

IV. DISCUSSION

We have demonstrated a method for measuring laser spark ignition energies and have shown that pulse duration (< 15 ns) and wavelength (355 nm $\leqslant \lambda \leqslant$ 1064 nm) are not significant properties of the ignition process, at least compared to the differences between laser spark and electric-discharge results. The laser pulse durations employed in this work are much shorter than the kinetic time scale for combustion chemistry. We can therefore view the laser spark as an instantaneous source of ignition energy, in contrast to the much longer duration of an electric-discharge spark. The following discussion proceeds with this fundamental assumption.

The properties of the source energy for ignition by laser-induced sparks and electric-discharge differ in many ways, especially in terms of (1) energy density and duration, (2) dissipation processes, and (3) geometry. All three properties (among many others) are inextricably coupled; we shall focus primarily on the interdependence of (1) and (2). The initiation of a flame requires localizing a sufficient amount of energy to heat a minimum flame volume to some threshold temperature. However, since an induction time τ is associated with ignition,[31,32] energy dissipation processes can play a critical role in the initiation and extinction of an incipient flame. Consequently, one can identify an optimum power density for flame ignition.

Recently, the interplay of critical energy and power distribution was modeled for the process of gaseous detonations by direct blast-wave initiation.[33–35] In these models, a condition is defined in which the blast-wave velocity has to exceed a critical shock velocity for a period of time that is longer than the induction time for combustion. Blast waves decay rapidly; therefore, the initiation occurs in a highly turbulent environment. The related problem of flame initiation requires the deposition of source energy (in addition to the heat of combustion) in proportion to the growth of the flame surface. If the duration of the energy source is too long (low power), then dissipation will compete with heating and the flame will extinguish. Likewise, too short a heating period (high power) can lead to excessively high initial temperatures, which can give rise to high-pressure blast waves that dissipate energy in a fast moving wave that does not couple effectively with the emerging combustion wave.

The threshold condition for flame initiation is defined as the temperature at which the heat of combustion offsets heat that is lost, due to cooling, to the surrounding cold gas or by flame stretch resulting from the surface area of the expanding spherical flame front. In the absence of these loss mechanisms, the threshold temperature can be associated with the autoignition point. For H_2/air under ambient conditions, this occurs at about 800 K with an induction time on the order of 1 s.[36] For a spatially localized spark energy source, dissipation will limit the time that the energy or heat will remain within the relevant dimensions of the minimum flame kernel. One must put in sufficient energy to make τ less than the time for heat loss. Hence, a higher temperature must be reached in a shorter time in order to initiate combustion. In Fig. 6, we have represented the dependence of τ on temperature as a function of the fuel mixture ratio for H_2/air. The induction time contours were derived from calculations and parametrized equations of Oran *et al.*[37,38]

A. Homogeneous hot-gas model

The initiation of a flame requires localizing a sufficient amount of energy to heat a minimum flame volume to some threshold ignition temperature. We begin with a very simple model for source heating[2] which assumes that the energy is deposited homogeneously in a spherical volume of radius r. The volume temperature as a function of energy E can be expressed by

$$T = T_0 + E\left[(4\pi/3)r^3 c_p \rho_0\right]^{-1}, \tag{1}$$

where T_0 is the initial temperature, and c_p and ρ_0 are the heat capacity and density, respectively, of the ambient gas mixture. Ideally, ρ_0 should be allowed to vary with temperature. Calculated isotherms as a function of source energy for a

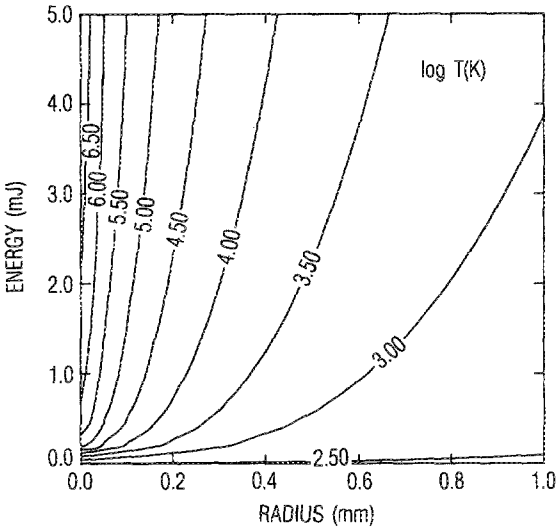

FIG. 7. Calculated isotherms as a function of source energy and volume radius for H_2/air initially at 1 atm and 300 K. The model assumes a homogeneous hot gas.

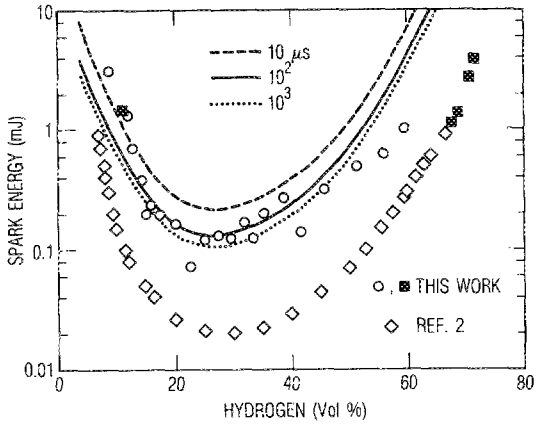

FIG. 8. Comparison of observed and calculated minimum ignition energies for H_2/air. The observed data are for 355-nm ns (■) and 532-nm ps (○) laser-induced spark ignition and represent the average of the lowest ignition energy and highest nonignition energy results from Fig. 3. Electric-discharge results (◇) are from Ref. 2. The curves represent calculated minimum ignition energies, assuming a homogeneous hot-gas model for H_2/air at 1 atm and 300 K and various induction times.

spherical volume of stoichiometric H_2/air are illustrated in Fig. 7.

A minimum ignition energy may be derived by identifying the minimum temperature and flame kernel radius for ignition. The latter quantity may be related to measured quenching distances[2] d_q (i.e., $r_{ig} = d_q/2$). The value of d_q is proportional to the preheat zone thickness and, hence, becomes greater away from stoichiometry as well as for increasing pressure and turbulence.[1,2] The ignition temperature T_{ig} is a function of the chemical induction time and, hence, depends on the time scale for dissipation. Without adopting a specific model for dissipation at this time, we can derive an approximate expression for ignition energies by determining the temperature for which the chemical induction time τ is comparable or less than the characteristic decay time for dissipation. Rearranging Eq. (1) then gives

$$E_{ig}(\tau) = (\pi/6) d_q^3 c_p \rho_0 [T_{ig}(\tau) - T_0], \tag{2}$$

where all terms except T_0 vary with the fuel mixture ratio. A more accurate expression should average $E_{ig}(t)$ over time, e.g.,

$$E_{ig} = \int_0^\infty E_{ig}(t') f(t',\tau) dt', \tag{3}$$

where $f(t',\tau)$ is a temporal distribution function for dissipation over the relevant geometry of the flame kernel. However, for our purposes, the simple relation given by Eq. (2) will suffice.

The calculated ignition energies as a function of fuel mixture ratio are compared to the experimental data in Fig. 8. The calculated curves are not a very sensitive function of induction time over the range considered. This is the inverse of the statement that the induction time (i.e., the kinetics for combustion) is very sensitive to temperature and energy, which is due to the large activation energy for combustion. The excellent agreement between the calculated and observed laser-induced spark ignition energies by this simple model must be considered somewhat fortuitous in view of the rather different results obtained by electric discharge. Further refinements to the working model for flame initiation and their relevance to the two sets of experimental data are discussed shortly.

B. Blast-wave model

We now consider a situation very different from the homogeneous hot-gas model, namely the instantaneous point-source deposition of energy. This treatment is somewhat representative of laser-induced sparks that require high power thresholds to induce breakdown ($\sim 10^{13}$ W/cm^2).[8] Short pulse durations are used to minimize spark energy. The instantaneously high pressures created by the tightly focused laser spark can be modeled as a Taylor blast-wave process.[39] The relevant time-dependent equations of state for the spherical shock can be expressed as[17,39]

$$r = (E/\rho_0)^{1/5} t^{2/5}, \tag{4}$$

$$v = \tfrac{2}{5}(E/\rho_0)^{1/2} r^{-3/2}, \tag{5}$$

$$P = [2/(\gamma+1)]\rho_0 v^2, \tag{6}$$

$$T = T_0\left[\left(1 - \frac{v_0^2}{v^2}\right)\left(\frac{\gamma-1}{\gamma+1}\right) + 1\right] \times \left[\left(\frac{v^2}{v_0^2} - 1\right)\left(\frac{\gamma-1}{\gamma+1}\right) + 1\right], \tag{7}$$

where v and v_0 are the shock and sonic velocities, respectively, $\gamma = c_p/c_v$, and P and T represent peak pressure and temperature, respectively. Other terms have been defined previously. The time evolution of these properties is illustrated for stoichiometric H_2/air as a function of spark energy in Figs. 9 and 10.

A blast wave can ignite a mixture either directly or by the force of the shock wave or by the hot gas that remains after the expansion. For the low-energy sparks considered in this work, the Taylor expansion is very short lived (Fig. 9). We can define a criterion for direct ignition on the basis of maintaining a peak temperature T that exceeds the threshold ignition T_{ig} for a time longer than the induction time. This is analogous to conditions established for direct initiation of

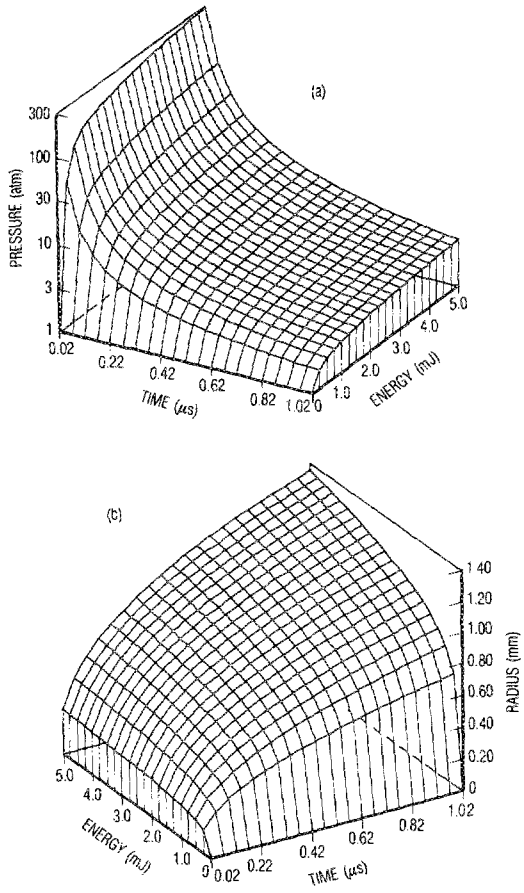

FIG. 9. Calculated time evolution for (a) pressure and (b) radius assuming a Taylor blast-wave model for a tightly focused laser-induced spark. Calculation assumes a stoichiometric H_2/air mixture at 1 atm and 300 K.

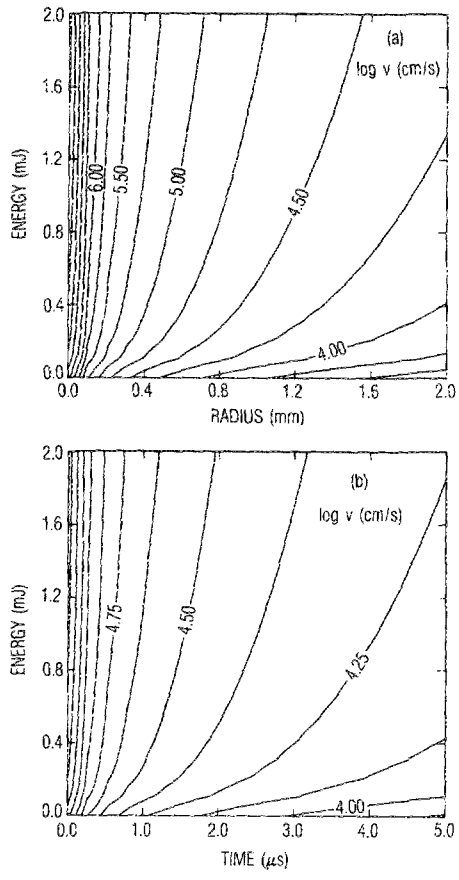

FIG. 10. Calculated blast-wave velocity contours as a function of (a) energy and radius and (b) energy and time. Calculation assumes a stoichiometric H_2/air mixture at 1 atm and 300 K.

detonations where a threshold shock velocity, rather than a temperature, was identified.[19,33–35,40] It can be readily shown, by observing the very rapid decay of the blast-wave temperature, that energies ($> 10^3$ mJ for stoichiometric H_2/air at 1 atm) far in excess of the observed ignition energies are required for direct initiation.

If one ignores the initial shock of the blast wave, then the heat generated by the expansion after the blast-wave front has decayed to near ambient conditions should be available for ignition. If the blast wave completely relaxes on a time scale that is short compared to the induction time for combustion, then one might expect the heated gas to efficiently ignite the mixture in a manner similar to the hot-gas model (Fig. 8). However, two effects argue against this being the case: (1) the blast-wave energy is typically dissipated over dimensions greater than the minimum flame volume, and (2) the blast front is still moving with significant velocity over times that are comparable to combustion. These points are supported by the blast-wave velocity calculations represented in Fig. 10. First, according to Fig. 10(a), the blast wave continues to expand outside of the minimum flame volume for relevant spark energies, thereby removing energy from this critical kernel. The ignition model assumes that a threshold energy density must be reached *within* the minimum flame kernel. Consequently, the proportion of energy lost in the expansion of the blast wave must be compensated by increasing the initial source energy. Second, the time scale for the expansion is comparable to typical induction times and, hence, can cause a turbulent disturbance that can extinguish a fragile minimal flame. According to Fig. 10(b), the blast wave is calculated to be supersonic only over very short times (1.5 μs for a 1-mJ spark), however, substantial velocity remains for much longer times ($\sim 10^4$ cm/s at 5–10 μs for a 1-mJ spark). Although the simple blast-wave model is qualitative for subsonic conditions, the possibility for turbulent disturbance[11,12,41] at these low energies cannot be ignored. Furthermore, recompression effects from the collapsing blast-wave may prolong disturbances over longer and more important time scales.

C. Chemical energy release

The presence of blast-wave disturbances in the ignition process by laser-induced sparks would be consistent with the higher ignition energies measured relative to earlier electric-discharge results[2] (Figs. 3 and 8). On the other hand, the present measurements conform nicely with calculated minimum ignition energies, using the ideal hot-gas model. Furthermore, earlier workers have had difficulty explaining the unexpectedly low ignition energies measured by electric discharge.[2] Explanations have included the possibility of catalytic surface effects at the electrodes,[19] as well as contributions to the total energy due to the heat of combustion.[2] We explore the second possibility by calculating the available reaction enthalpy in a minimal flame, assuming complete

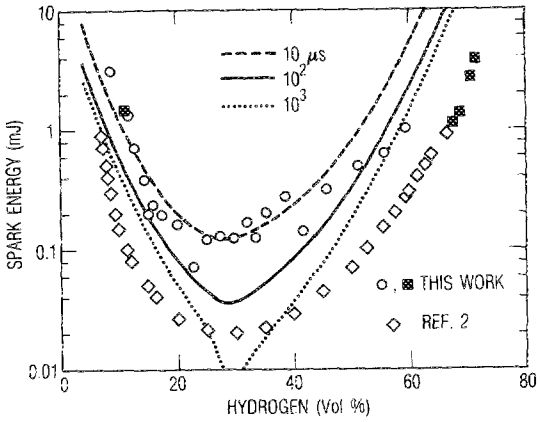

FIG. 11. Comparison of observed and calculated minimum ignition energies for a homogeneous hot-gas model, including chemical energy release. Symbols and experimental conditions are described in the caption to Fig. 8.

combustion within the flame core.

The available combustion energy is computed using the enthalpy associated with the net reaction $H_2 + \frac{1}{2}O_2 \rightarrow H_2O(g)$ ($\Delta H = -241.83$ kJ/mol) and the molar content of reactants in a minimum flame kernel as a function of fuel ratio. No allowance is made for the high diffusivity of H_2 which replenishes burned H_2 in the early spherical flame, thereby favoring ignition to the lean side of stoichiometry, nor has the energy of activation been rigorously considered. Modified ignition energies are calculated by subtracting the maximum available chemical energy from the total energy calculated by the hot-gas model. The results are plotted along with the experimental data in Fig. 11. The simple model used here introduces an artificial lowering of E_{ig}, especially for long induction times near stoichiometry where the exothermicity of the reaction approaches the hot-gas model ignition energy. This occurs because we have not explicitly included the energy of activation, which prevents the mixtures from self-igniting. In spite of the underestimations of the calculated ignition energies, the measured values by electric-discharge still occur at lower energy over much of the range of fuel ratios.

The inability to explain the low electric-discharge energy thresholds may be attributable to a variety of effects. For instance, agreement can be obtained if we reduce the assumed minimum flame volume in proportion to the discrepancy. However, the appropriate volumes are based on measured quenching distances, which are considered in the literature to be very reliable ($\sim \pm 10\%$).[1] Another possibility is that small turbulences by low-energy electric discharge can promote burning velocities, thereby reducing the necessary ignition energy.[11,12] (For greater turbulence, the preheat zone thickness increases, ultimately raising the necessary ignition energy.) Finally, it may be argued that catalytic effects involving the electrode surfaces may contribute to the ignition efficiency.[19] Naturally, a combination of these and other effects may be implicated.

V. SUMMARY AND CONCLUSIONS

We have established that ignition energy measurements by laser-induced spark initiation is a viable technique. No significant dependence on pulse duration (~ 10 ns vs ~ 30 ps; cf. Sec. II) or wavelength (355, 532, and 1064 nm) was observed. Although these properties influence the threshold for breakdown, once breakdown is achieved, ignition depends only on the amount of energy absorbed in the plasma. The laser pulse duration, unlike electric-discharge duration, is much shorter than the kinetic time scale and considerably shorter than the induction time for ignition and, hence, approximates an instantaneous and localized source of energy. We have not investigated the possibility of photochemical effects for specific wavelengths that might resonantly dissociate reactant molecules or excite radical intermediates.[21–25]

The laser-induced minimum ignition energy curve as a function of H_2/air ratio is approximately parallel to electric-discharge results, although larger by a factor of about 5 at stoichiometry. (The discrepancy decreases for higher H_2/air ratios.) A similar trend was observed for hexane/air; no available electric-discharge data for 1,1'-dimethyl hydrazine is available for comparison. Several characteristic properties that distinguish laser-induced sparks from electric-discharge ignition were identified. Using simple models, it was concluded that the high-energy density and short duration of laser-induced sparks is less efficient for flame initiation than electric-discharge. The following observations can be made:

(1) The initiation of a flame requires localizing a sufficient amount of energy to heat a minimum flame volume to some threshold ignition temperature.

(2) The induction time for combustion increases with decreasing temperature; hence, minimum ignition energies are favored by conditions that permit long residence times for energy deposition in the minimum flame volume.

(3) The optimum heating rate for facilitating ignition is balanced by the benefit of a long induction time (i.e., lower threshold temperature) and the disadvantage of dissipative heat loss. (Favorable energy source durations for stoichiometric H_2/air are estimated to be in the 1–100 μs range depending on mixture composition.)

(4) An optimum power density can be identified; excessive values can cause blast-wave losses and turbulent disturbances that can disrupt the natural evolution of the spherical flame.

The lower ignition energies measured by electric discharge compared to the present laser-induced sparks results can be explained by the electric energy source satisfying the condition (3) and the laser source suffering from condition (4). Moreover, it can be argued that the elongated energy distribution characteristic of electric discharge permits a more favorable cylindrical rather than spherical propagation during the critical early stages of the minimal flame.

In spite of these conditions, simple models for calculating the thermodynamic minimum ignition energy requirements are in good agreement with the laser-induced sparks results, but are incapable of accounting for the low electric-discharge energy thresholds. Agreement can be reached if we reduce the assumed minimum flame volume in proportion to the discrepancy, although reliable measurements of quenching distance exist to refute this possibility. Other possible explanations for the low electric-discharge energy

thresholds include (1) small turbulences which promote burning velocities, thereby reducing the necessary ignition energy,[11,12] and (2) catalytic effects involving the electrode surfaces that may contribute to the ignition efficiency.

ACKNOWLEDGMENTS

We wish to recognize the individuals who contributed valuable electronics and software support. Charles Colborne was exceptionally productive in developing software and interface components for instrument control and providing general electronics troubleshooting skills. Robert Hertz was very helpful in the construction of the digital control unit used to automate the apparatus. Finally, we wish to acknowledge valuable discussions with Dr. Tom Spiglanin, Dr. Ed Beiting, and Dr. Tom Knudtson. This work was funded by the Aerospace Sponsored Research Program.

[1]R. A. Strehlow, *Combustion Fundamentals* (McGraw-Hill, New York, 1984).
[2]B. Lewis and G. Von Elbe, *Combustion, Flames and Explosions of Gases*, 2nd ed. (Academic, New York, 1967).
[3]J. E. M. Goldsmith and R. J. M. Anderson, Opt. Lett. **11**, 67 (1986).
[4]J. E. M. Goldsmith and N. M. Laurendeau, App. Opt. **25**, 276 (1986).
[5]M. G. Allen, R. D. Howe, and R. K. Hanson, Opt. Lett. **11**, 126 (1986).
[6]J. M. Seitzman, G. Kychakoff, and R. K. Hanson, Opt. Lett. **10**, 439 (1985).
[7]M. J. Dyer and D. R. Crosley, Opt. Lett. **7**, 382 (1982).
[8]M. Aiden, H. Edner, G. Holmstedt, S. Svanberg, and T. Hogberg, Appl. Opt. **21**, 1236 (1982).
[9]N. S. Bergano, P. A. Jaanimagi, M. M. Salour, and J. H. Bechtel, Opt. Lett. **8**, 443 (1983).
[10]S. Stepowski and M. J. Cottereau, Combust. Flame **40**, 65 (1981).
[11]D. R. Ballal and A. H. Lefebvre, Combust. Flame **24**, 99 (1975).
[12]D. R. Ballal and A. H. Lefebvre, Proc. R. Soc. London Ser. A **357**, 163 (1977).
[13]Yu. P. Raizer, *Laser-Induced Discharge Phenomena* (Consultants Bureau, New York, 1977).
[14]N. Yackerson and N. S. Kopeika, IEEE J. Quantum Electron. **QE-21**, 1964 (1985), and references therein.
[15]R. G. Kingdon and F. J. Weinberg, *Sixteenth Symposium on Combustion* (Combustion Institute, Pittsburg, PA, 1977), p. 747.
[16]R. A. Hill and G. A. Laguna, Chem. Phys. Lett. **32**, 435 (1980).
[17]R. W. Schmieder, J. Appl. Phys. **52**, 3000 (1981).
[18]B. E. Forch and A. W. Miziolek, Combust. Sci. Technol. **52**, 151 (1987).
[19]J. H. Lee and R. Knystautas, AIAA J. **7**, 312 (1969).
[20]F. J. Weinberg and J. R. Wilson, Proc. R. Soc. London Ser. A **321**, 41 (1971).
[21]J. H. Lee, R. Knystautas, and N. Yoshikawa, Acta Astronaut. **5**, 971 (1978).
[22]M. E. Levy, A. E. Cerkanowicz, and R. F. McAlevy, AIAA J. **7**, 1 (1969).
[23]M. Lavid and J. G. Stevens, Combust. Flame **60**, 195 (1985).
[24]B. E. Forch and A. W. Miziolek, Opt. Lett. **11**, 129 (1986).
[25]A. W. Miziolek and M. A. DeWilde, Opt. Lett. **9**, 390 (1984).
[26]D. Giulietti, A. Giulietti, M. Lucchesi, and M. Vaselli, J. Appl. Phys. **58**, 2916 (1985).
[27]J. A. Syage, R. Rianda, E. W. Fournier, and R. B. Cohen, *Proceedings of the 24th JANNAF Combustion Meeting* (CPIA Publication, in press).
[28]C. M. Guirao, G. G. Bach, and J. H. Lee, Combust. Flame **27**, 341 (1976).
[29]H. M. Thompson, J. W. Daiber, and R. G. Rehm, J. Appl. Phys. **47**, 2427 (1976).
[30]J. A. Syage, E. W. Fournier, and R. B. Cohen (unpublished).
[31]C. H. Yang and B. F. Gray, J. Phys. Chem. **73**, 3395 (1969).
[32]C. H. Yang, J. Phys. Chem. **73**, 3407 (1969).
[33]J. H. S. Lee, Ann. Rev. Phys. Chem. **28**, 75 (1977).
[34]R. Knystautas and J. H. Lee, Combust. Flame **27**, 221 (1976).
[35]G. E. Abouseif and T. Y. Toong, Combust. Flame **45**, 39 (1982).
[36]D. R. Stull, *Fundamentals of Fire and Explosion* (American Institute of Chemical Engineering, New York, 1977).
[37]E. S. Oran, T. R. Young, J. P. Boris, and A. Cohen, Combust. Flame **48**, 135 (1982).
[38]E. S. Oran and J. P. Boris, Combust. Flame **48**, 149 (1982).
[39]G. I. Taylor, Proc. R. Soc. London Ser. A **201**, 175 (1950).
[40]J. H. Lee and K. Ramamurthi, Combust. Flame **27**, 331 (1976).
[41]S. L. Aly and C. E. Hermance, Combust. Flame **40**, 173 (1981).